

# CONCEPTUAL AIRCRAFT DESIGN BASED ON LIFE CYCLE ASSESSMENT

**Andreas Johanning, Dieter Scholz**  
**Aircraft Design and Systems Group (AERO), Hamburg University of Applied Sciences,**  
**Hamburg, Germany**  
*andreas.johanning@haw-hamburg.de; info@ProfScholz.de*

**Keywords:** *Conceptual Aircraft Design, Life Cycle Assessment*

## Abstract

*This paper investigates the influence of the integration of Life Cycle Assessment (LCA) on conceptual aircraft design. The Environmental Impact (EI) of different life cycle phases and the driving design parameters of the EI of an aircraft are analyzed. A trade-off between low EI and low Direct Operating Costs (DOC) is investigated. It is shown that while DOC and EI optimized aircraft differed a lot in the past when Airbus A320 had its entry into service, they have nowadays become more similar due to a strong surge of fuel price making low fuel consumption a key design criterion also for DOC. It is shown that in 2030, a next generation turboprop driven medium range aircraft, solely optimized for minimum EI, could have the potential of improving EI by about 46 % while still improving DOC by about 12 % compared to nowadays medium range aircraft.*

## 1 Introduction

### 1.1 Motivation

Several organizations attempt to reduce the EI of civil aviation by setting objectives for the reduction of CO<sub>2</sub> emissions [1]. CO<sub>2</sub> emissions are proportional to the amount of fuel burned. Therefore CO<sub>2</sub> emissions could be reduced by reducing the fuel consumption of aircraft for instance by optimizing aircraft for minimum fuel consumption. In a more comprehensive approach, aircraft could be optimized for minimum EI not only considering CO<sub>2</sub>

emissions during aircraft operation but also other emissions occurring during the entire aircraft life cycle and their actual EI. The calculation of the EI can be performed with a Life Cycle Assessment which is defined as the „compilation and evaluation of the inputs, outputs and the potential EIs of a product system during its life cycle” [2].

At the German Aerospace Conference in 2013, a methodology has been presented allowing to integrate a simplified LCA into conceptual aircraft design. [3] Based on that methodology, this paper investigates the influence of the integration of LCA on conceptual aircraft design using a Turboprop driven Aircraft (TA) as design example. As shown in [4], such an aircraft might be a potential candidate for the future medium range aircraft generation and therefore suits perfectly as design example.

The outline of the paper is as follows. Section 2 analyzes the EI of each life cycle phase to investigate the percentage of each phase on the overall EI. Section 3 presents how the introduction of the EI as a design objective changes the design of an aircraft. Section 4 investigates the driving design parameters of the EI of an aircraft. Section 5 investigates the trade-off between low EI and low DOC using a Pareto front analysis while Section 6 concludes the paper.

### 1.3 Reference Aircraft and Reference Mission

The reference aircraft for evaluating the performance of the TA design is the weight

variant WV000 of the Airbus A320-200 with CFM56-5A engines [5]. Key parameters of the selected weight variant are listed in Table 1. A three-view drawing is shown in Fig. 1.

Table 1. Key parameters of the selected A320-200 weight variant from [5]

Parameter	A320
$m_{MTO}$ [kg]	73500
$m_{OE}$ [kg]	41244
$m_{MPL}$ [kg]	19256
$R_{MPL}$ [NM]	1510
$n_{PAX}$ (1-cl HD) [-]	180
$M_{CR}$ [-]	0.76

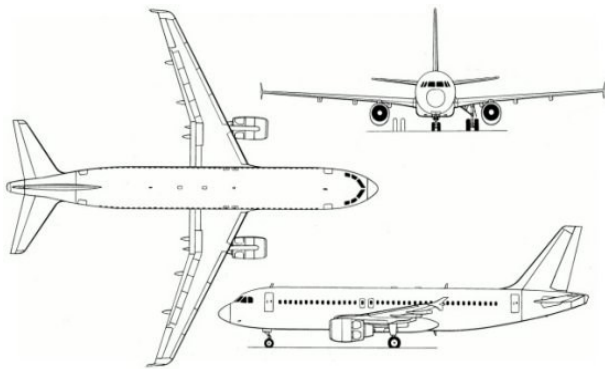


Fig. 1 Three-view drawing of the Airbus A320-200 [6]

The proposed TA has the same requirements as the reference aircraft except that a lower cruise Mach number is allowed to take account of the speed limitations of TA.

## 2 Environmental Impact of Different Life Cycle Phases

In a first step, the EI of each life cycle phase will be analyzed to investigate the percentage of each phase on the overall EI. Additionally, the most important processes contributing to the EI will be determined.

The presented results are based on an analysis of the reference aircraft using the methodology presented in [3]. The total EI of an aircraft is expressed by the so called Single Score (SS). The lower SS, the lower the total EI of the aircraft.

As shown in Fig. 2, the operational phase completely dominates the EI of the reference aircraft with a contribution of 99.8 % to the SS. The production follows with a contribution of

about 0.2 % while design and development have a minor contribution of about 0.0007 %.

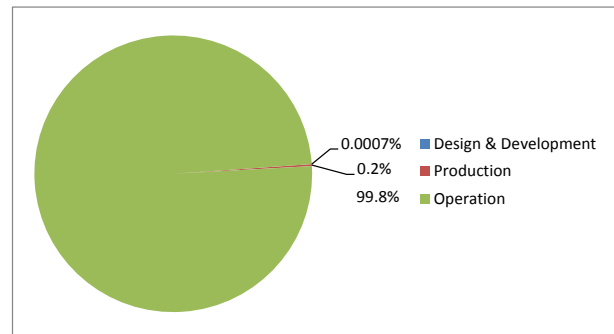


Fig. 2. Contribution of the life cycle phases to the SS of the reference aircraft

Fig. 3 shows the contribution of different processes within the life cycle to the SS. It can be seen that kerosene production is responsible for about 50 % of the SS, followed by the burning of fuel during the flight (represented by the processes “Cruise flight” and “LTO-cycle”) which contributes another 48 % to the SS. The operation of airports (represented by the processes “Energy generation and consumption at airports” and “Ground handling”) contributes another percent to the SS.

Roughly 98 % of the SS are directly caused by the fuel consumption of the aircraft which indicates that minimizing fuel consumption is essential for also minimizing EI.

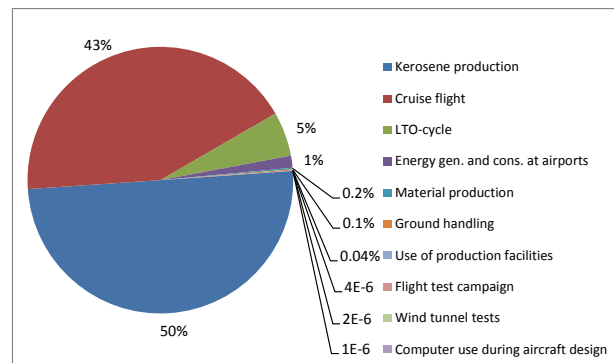


Fig. 3. Contribution of processes to the SS of the reference aircraft

As expected, the results show that the main contribution to the EI of an aircraft comes from the operational phase which accounts for more than 99 % of the total EI. In that phase the production and combustion of fuel account for most part of the impact. Therefore reducing the

amount of fuel burned is of highest importance for low EI.

### 3 Influence of Life Cycle Assessment on Conceptual Aircraft Design

In this section, it will be presented how the introduction of the EI as a design objective changes the design of an aircraft. During design optimization, the following seven design parameters have been optimized for minimum EI: landing field length  $s_{LFL}$ , ratio of maximum landing mass to maximum take-off mass  $m_{ML}/m_{MTO}$ , cruise Mach number  $M_{CR}$ , effective wing aspect ratio  $A_{W,eff}$ , wing sweep at 25 % chord  $\phi_{25}$ , wing thickness ratio  $t/c$  and propeller diameter  $d_{prop}$ .

Take-off field length  $s_{TOFL}$  has been kept constant and set equal to the value of the reference aircraft. For the optimization of  $s_{LFL}$ , the value of  $s_{TOFL}$  has been set as upper limit. Aircraft usually require slightly shorter  $s_{LFL}$  than  $s_{TOFL}$ . Therefore it makes sense to set  $s_{TOFL}$  to the allowable upper limit and to set the value of  $s_{LFL}$  free.

The determined optimum wing taper ratio for minimum EI has always been located at its lower limit. The advantage of a lighter wing at lower taper ratio always overcompensated the disadvantage of a sometimes lower glide ratio due to a not optimum lift distribution over the wing. Later, during optimization, taper ratio has therefore been set to the lower limit of 0.2 because this is the suggested minimum allowable taper ratio according to [7].

To optimize the aircraft for minimum EI, the value of SS introduced in the previous section has been minimized using an evolutionary algorithm with a population size of 35 and 60 generations. Afterwards, the design results have been compared to the redesign results of the reference aircraft.

For all aircraft design investigations within this paper, the aircraft design software PrOPerA developed by the Aircraft Design and Systems Group (AERO) has been used.

The designs have been evaluated for an entry into service in 2030 when the next generation of medium range aircraft might be

introduced. For that year, an inflation-adjusted fuel price of 1.32 USD/kg has been assumed based on the method proposed in [8]. The reference aircraft has been evaluated with the same fuel price to have a fair comparison in the year 2030.

As potential candidate for a next-generation medium range aircraft, a turboprop driven aircraft including the future technologies Strut Braced Wing (SBW) and Natural Laminar Flow (NLF) has been selected.

Fig. 4 presents the results of the aircraft design optimization. The Figure contains a three- and a 3D-view, the most important aircraft requirements and parameters, a payload-range and DOC-range diagram, a matching chart, a cross-section of the cabin as well as breakdowns for operating empty mass, drag and DOC.

The resulting aircraft design, solely optimized for minimum EI, has a significantly lowered cruise Mach number of 0.4 which has been set as lower limit for the optimizer.

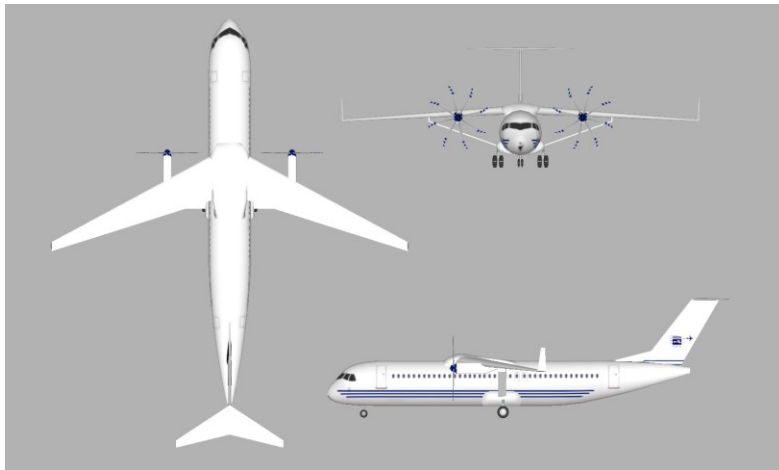
A 20 % reduction of the wing area enabled by the lower total aircraft mass allows to have a strong increase of the effective wing aspect ratio without exceeding the required maximum wing span of 36 m to stay within the code letter C requirements of airports [9].

The high propeller diameters cause small propeller disc loadings leading to high propeller efficiencies.

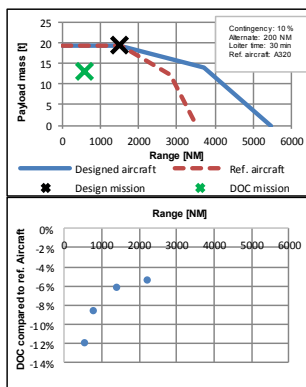
Altogether, fuel savings of 43 % can be achieved on the design mission. Together with additional snowball effects, this leads to a 25 % reduction of maximum take-off mass.

On the DOC mission, such an aircraft design offers the potential of reducing the EI by about 46 % while DOC could still be reduced by about 12 %.

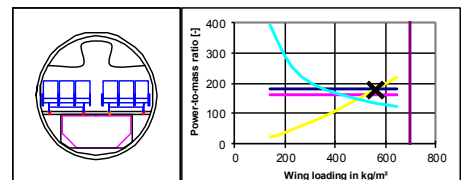
At first glance, the achievable DOC improvements seem to be a surprise because nowadays medium range aircraft fly at much higher Mach numbers allowing to fly more passenger-kilometers in a certain time. But due to the fact that rising fuel costs increasingly dominate the DOC, low fuel consumption becomes a more and more important design criterion while high cruise speeds loose importance.



Parameter	Value	Deviation from A320*
<b>Requirements</b>		
$m_{MPL}$	19256 kg	0 %
$R_{MPL}$	1510 NM	0 %
$M_{CR}$	0.40	-47 %
$\max(s_{TOFL}, s_{LFL})$	1770 m	0 %
$n_{PAX}$ (1-cl HD)	180	0 %
$m_{PAX}$	93 kg	0 %
$SP$	29 in	+0 %



Parameter	Value	Deviation from A320*
<b>Main aircraft parameters</b>		
$m_{MTO}$	55100 kg	-25 %
$m_{OE}$	28400 kg	-31 %
$m_F$	7500 kg	-43 %
$S_W$	99 m <sup>2</sup>	-19 %
$b_{W,geo}$	36.0 m	+6 %
$A_{W,eff}$	14.6	+54 %
$E_{max}$	20.0	≈ +14%
$P_{eq,ssl}$	5000 kW	-----
$d_{prop}$	6.5 m	-----
$\eta_{prop}$	88 %	-----
$PSFC$	5.87E-8 kg/W/s	-----
$h_{ICA}$	14000 ft	-63 %
$s_{TOFL}$	1770 m	0 %
$s_{LFL}$	1720 m	+19 %
$t_{TA}$	32 min	0 %



Parameter	Value	Deviation from A320*
<b>DOC mission requirements</b>		
$R_{DOC}$	589 NM	0 %
$m_{PL,DOC}$	13057 kg	0 %
EIS	2030	-----
$C_{fuel}$	1.32 USD/kg	0 %
<b>Results</b>		
$m_{F,trip}$	2500 kg	-45 %
$U_{a,f}$	3030 h	+10 %
DOC (AEA)	88 %	-12 %
SS	0.0043	-46 %

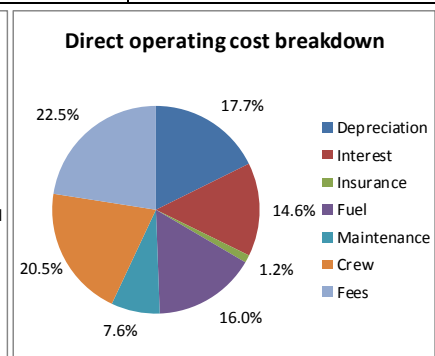
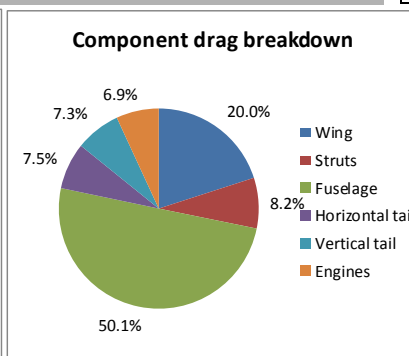
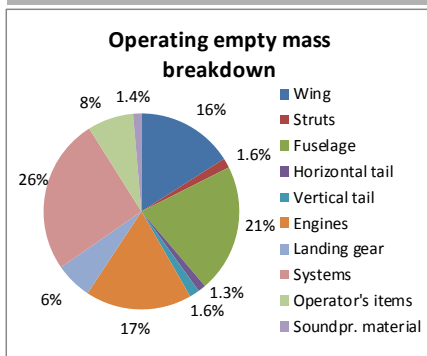


Fig. 4. Design results of the EI optimized aircraft

The EI optimized aircraft has such a low  $M_{CR}$  because it lowers the requirement for the power-to-mass ratio of the engine at a given wing loading allowing to have smaller and lighter engines helping to reduce fuel consumption. Interestingly, looking at the matching chart in Fig. 4, the requirement from  $M_{CR}$  for the power-to-mass ratio is lowered even below the dimensioning requirement coming from the 2<sup>nd</sup> segment.

First, this is because the lower  $M_{CR}$  and the lower the cruise altitude, the lower the fuselage mass causing additional snowball effects and again lower fuel consumption. Secondly, the lower  $M_{CR}$ , the higher the Oswald factor improving the glide ratio and also lowering fuel consumption.

In the matching chart, the landing requirement is not dimensioning either which will be discussed in Subsection 4.1.

In contrast to that, a DOC optimized aircraft often has landing, take-off and cruise line cutting through the design point so that all these requirements are dimensioning (cf. Fig. 5).

Fig. 6 shows a three-view of such a TA design with the same requirements as the TA above but optimized for minimum DOC. It can be seen that the aircraft is optically similar to that optimized for minimum EI. The main difference is the lower sweep angle of the wing and the tail. The trade-off between DOC and EI optimized aircraft is analyzed more detailed in Section 5.

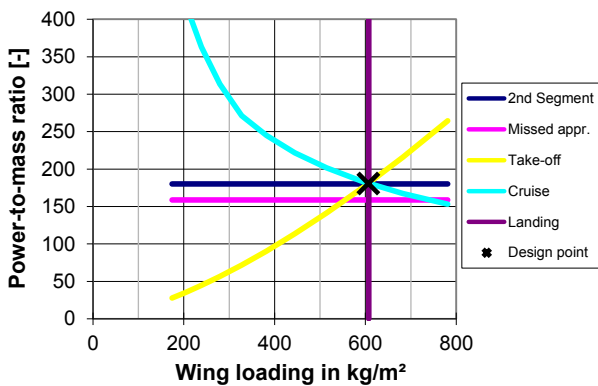


Fig. 5 Matching chart of a TA optimized for minimum DOC

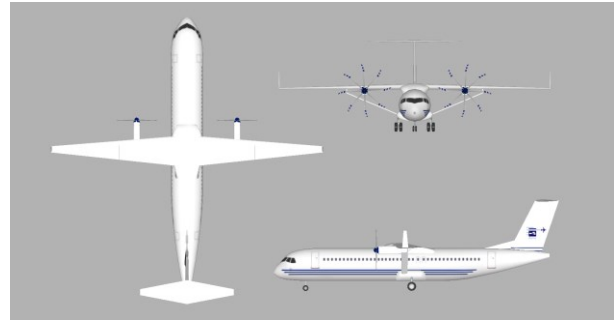


Fig. 6 Three view of a TA optimized for minimum DOC

## 4 Analysis of Sensitivity and Robustness

### 4.1 Sensitivity analysis

In this section, the respective importance of the optimized design parameters for EI will be analyzed using a sensitivity analysis and it is investigated how these design parameters influence the EI in conceptual aircraft design.

All design parameters have been varied in a range of - 50 % ... + 50 % around their determined optimum value (from the previous section) and the influence on EI has been calculated. The results of that analysis are presented in the following Figures. Each point represents a converged aircraft design. If a design did not converge, no point is plotted so that some curves are not visible over the entire range. The curves of all design parameters will be discussed within the following paragraphs.

Fig. 7 shows the curve of  $A_{W,eff}$  which has a negative slope over its entire range. This means that the higher  $A_{W,eff}$ , the lower EI. In the optimization,  $A_{W,eff}$  is limited by the required maximum wing span of 36 m. Above the determined optimum  $A_{W,eff}$  the designs are infeasible because they do not fulfill the span requirement anymore. Without that requirement, lower EI could be reached by further increasing  $A_{W,eff}$ . During optimization,  $A_{W,eff}$  has been doubled compared to the reference aircraft. The Figure shows that this doubling alone leads to an EI improvement of roughly 30 %.

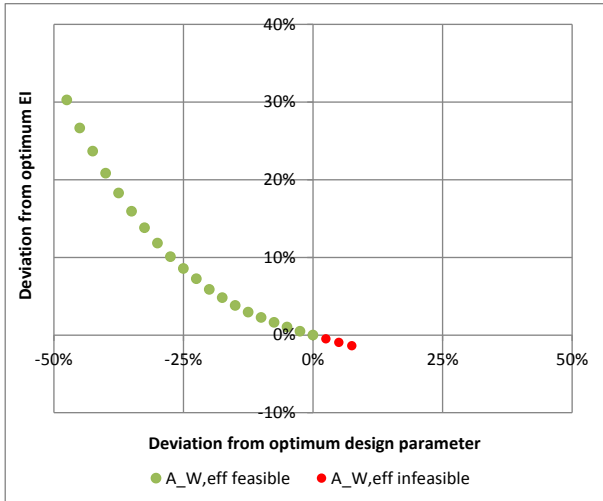
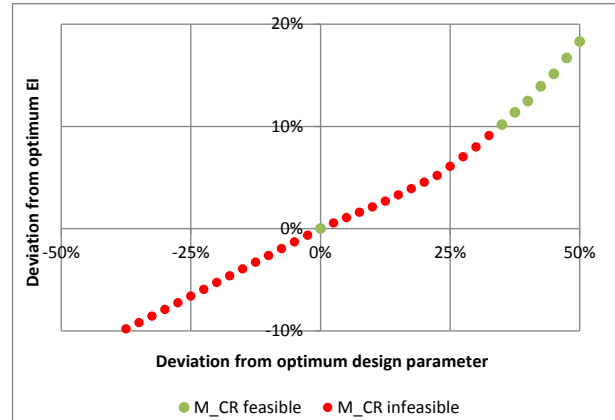

 Fig. 7 Sensitivity analysis of  $A_{W,eff}$ 

Fig. 8 shows the curve of  $M_{CR}$  which has a positive slope over the entire range of the curve. This means that the lower  $M_{CR}$ , the lower EI. The determined optimum  $M_{CR}$  is 0.4 which has been set as low limit for the optimization. Below that value, the designs are therefore infeasible even though EI could be reduced even more if the limit for the Mach number would be lowered. Above the value of 0.4, the designs are infeasible because the maximum span requirement is broken again. This is because higher Mach numbers lead to higher fuel consumption which finally leads to an increase of aircraft mass. For a given wing loading, this leads to a higher required wing area and for a given aspect ratio to a higher wing span.

When aircraft are optimized for lowest DOC, higher Mach numbers usually are advantageous because they lead to a higher number of flights in a certain time period even though lower Mach numbers can offer lower fuel consumption which is also positive for low DOC. In contrast to that, for low EI, low fuel consumption is of highest importance so that low cruise Mach numbers are preferable.


 Fig. 8 Sensitivity analysis of  $M_{CR}$ 

The designs with variations of  $d_{prop}$  are shown in Fig. 9. The curve first has a negative slope because propeller efficiency is improved with increasing  $d_{prop}$  lowering fuel consumption. But above a certain  $d_{prop}$  (which is below the optimum value),  $d_{prop}$  becomes dimensioning for the landing gear length leading to a heavier landing gear impairing fuel consumption and leading to a positive slope in the right part of the curve. The minimum value of the resulting curve in Fig. 9 is lying in the infeasible region below the optimum value of  $d_{prop}$ . The designs below the optimum  $d_{prop}$  do not fulfill the maximum span requirement because their take-off mass is too high. For a given wing loading and aspect ratio, this again requires a wing span above the upper limit of 36 m so that the designs become infeasible.

The designed aircraft have a main landing gear that is mounted on the fuselage and folded in lateral direction to the fuselage. The longer the landing gear, the further outside the landing gear legs have to be mounted. Above a certain  $d_{prop}$ , the required landing gear length is so high that the legs would have to be mounted unrealistically far outboard the fuselage so that the designs become infeasible again explaining the infeasible designs in the right part of the curve. By folding the main landing gear in longitudinal direction, even higher landing gear lengths could be realized. However it is acceptable to not consider this type of folding here because the optimum  $d_{prop}$  requires a shorter landing gear length anyway.

As a consequence of the previous considerations, only few designs in a short

range above the determined optimum  $d_{prop}$  are feasible.

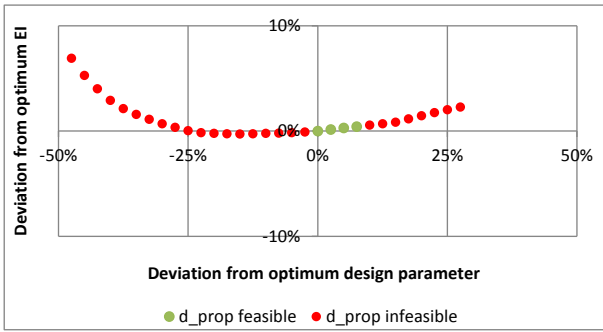


Fig. 9 Sensitivity analysis of  $d_{prop}$

Fig. 10 shows the sensitivity analysis of  $\varphi_{25}$ . It can be seen that the curve is falling until a value a little bit above the determined optimum value. In the right part, the curve is rising again. The course of the curve can be explained by the fact that the optimizer found an optimized taper ratio of 0.2 and a sweep angle of roughly  $25^\circ$  which together leads to an optimum lift distribution and therefore the highest Oswald factor. The value of the Oswald factor is increasing up to the determined optimum  $\varphi_{25}$  and is decreasing afterwards. With increasing Oswald factor, the glide ratio is improved causing additional positive snowball effects like a lower required power-to-mass ratio. The lower power-to-mass ratio leads to lighter engines to some extent balancing the mass increase of the wing due to higher  $\varphi_{25}$ . Above the determined optimum  $\varphi_{25}$ , the lift distribution is impaired again, Oswald factor and therefore glide ratio decrease so that fuel consumption, EI and take-off mass start to rise again.

As explained before, the increase of take-off mass finally also requires an increase of wing span. Above the determined optimum  $\varphi_{25}$ , the allowed limit is exceeded so that those designs are infeasible.

When optimizing for minimum DOC, the optimum  $\varphi_{25}$  would be very low at the given Mach number of 0.4. This is because in DOC optimization, the overall aircraft mass plays a more important role as it influences aircraft price and fees for instance (at least in the used AEA DOC method [10]). Reducing  $\varphi_{25}$  requires more fuel mass but lowers wing mass and therefore operating empty mass. Together, the

overall aircraft mass is reduced so that low  $\varphi_{25}$  would be preferable during DOC optimization.

In contrast to that, the EI optimized aircraft is a fuel mass optimized aircraft. The higher overall aircraft mass is of lower importance so that the optimizer prefers higher  $\varphi_{25}$ .

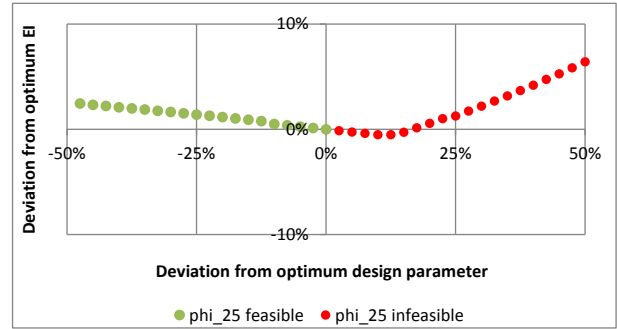


Fig. 10 Sensitivity analysis of  $\varphi_{25}$

The sensitivity analysis of  $t/c$  is shown in Fig. 11. It can be seen that a variation of  $t/c$  does not have much influence on EI. On the one hand, wing mass goes down with increasing  $t/c$  but on the other hand  $C_{D,0}$  increases impairing the glide ratio. Concerning their impact on EI both effects roughly balance each other below the determined optimum  $t/c$ . Above that value, the increase of  $C_{D,0}$  is dominating leading to a slightly positive slope of the curve.

Usually low  $t/c$  are also advantageous concerning wave drag. However this does not matter for the presented design because the cruise Mach number is very low.

Like in the other cases, below the determined optimum  $t/c$ , the wing span gets too high so that the designs are infeasible.

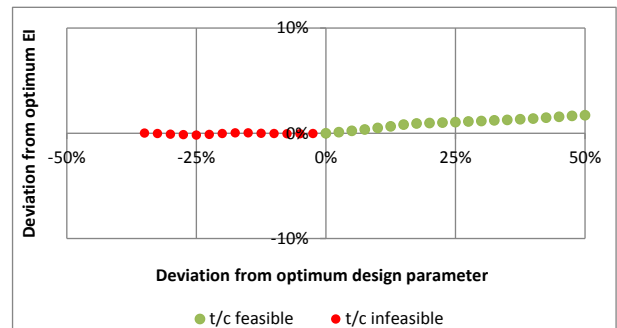


Fig. 11 Sensitivity analysis of  $t/c$

Fig. 12 shows the sensitivity analysis of  $m_{ML}/m_{MTO}$ . Interestingly, only one design at the determined optimum value for  $m_{ML}/m_{MTO}$  is feasible. Below, the actual landing mass would

be higher than the allowed maximum landing mass making the designs infeasible. Above, the maximum span requirement is broken again and there is a trend of impaired EI. This is because the higher  $m_{ML}/m_{MTO}$  leads to a higher allowed landing mass eventually requiring a bigger and heavier wing to fulfill the requirement coming from the maximum allowed landing field length as well as stronger and heavier engines to fulfill the missed approach requirement. Of course this depends on what requirements are dimensioning the design.

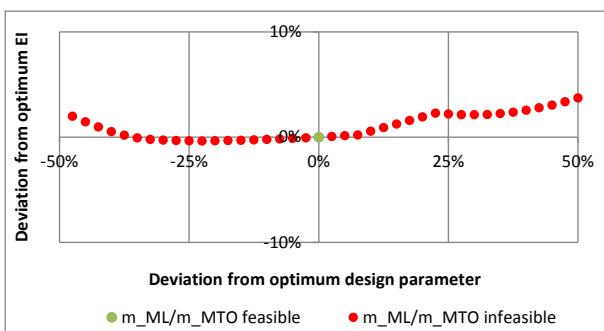


Fig. 12 Sensitivity analysis of  $m_{ML}/m_{MTO}$

Finally, the sensitivity analysis of  $s_{LFL}$  is presented in Fig. 13. It can be seen that EI is not very sensitive to changes of  $s_{LFL}$ . This is mainly because  $s_{LFL}$  is not a dimensioning criterion for the EI optimized TA as shown in the matching chart of Fig. 14. When designing aircraft for minimum DOC,  $s_{LFL}$  is often a dimensioning criterion so that changes of  $s_{LFL}$  strongly affect the design results. In contrast to that, when optimizing for minimum EI, the design point chosen by the optimizer was mostly located at the lowest possible power-to-mass ratio and the landing requirement was not dimensioning. The course of the curve can be explained by other advantages and disadvantages coming from the change of  $s_{LFL}$ :

Based on the equations within the design tool, the higher  $s_{LFL}$ , the higher the approach speed at landing, the higher the allowable stall speed in the landing configuration, the higher the stall speed in the take-off configuration, the higher the take-off speed, the higher the propeller efficiency during take-off. Therefore the slope of the curve representing the take-off requirement in the matching chart is a little bit less steep leading to higher allowable wing

loadings at a certain power-to-mass ratio. Therefore, increasing  $s_{LFL}$  leads to a slightly lower required wing area which makes the wings lighter and therefore helps to save fuel.

But the lower wing area increases the ratio of wetted area to wing area so that the zero-lift drag coefficient  $C_{D,0}$  is rising. The higher  $C_{D,0}$  lowers the achievable maximum glide ratio impairing the fuel consumption again.

Altogether, the disadvantages and advantages lead to an optimum compromise for  $s_{LFL}$  at about 1720 m. It has to be noted that the described effects are mild explaining the low sensitivity to changes of  $s_{LFL}$ .

Below the optimum  $s_{LFL}$ , the designs are infeasible because of the maximum span requirement. This is because wing area increases with decreasing  $s_{LFL}$ . Above a certain wing area, the span requirement is not fulfilled anymore for the given aspect ratio.

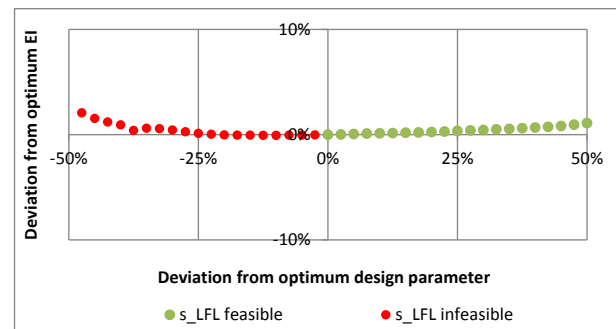


Fig. 13 Sensitivity analysis of  $s_{LFL}$

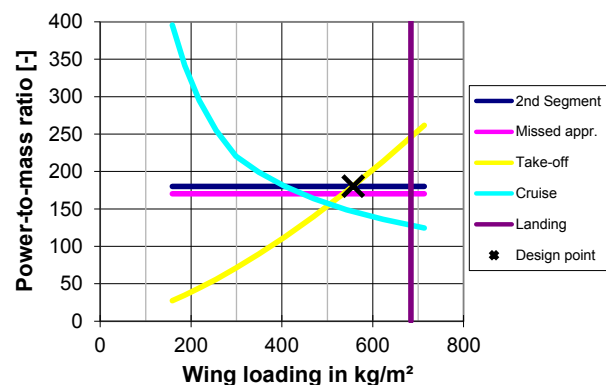


Fig. 14 Matching chart of the EI optimized TA

Looking at all sensitivity curves, it can be seen that EI is most sensitive to changes of  $A_{W,eff}$ . Therefore the first priority of the optimizer is to increase  $A_{W,eff}$  as much as possible. The second priority of the optimizer is to lower  $M_{CR}$  as much as possible. The priority

of all other design parameters is lower. They are adjusted to minimize EI but just enough that they still fulfill the maximum span requirement which strongly drives the entire design.

### 4.2 Robustness analysis

An analysis of the robustness of the performed optimization is presented in Fig. 15. Unlike in the previous subsection, the results of all varied parameters are plotted in a single diagram and infeasible designs are not marked separately. It can be seen that a separate variation of each design parameter between - 5 % ... + 5 % leads to changes of EI between about - 1 % ... + 1 %. There are no outliers or unexpected jumps around the optimum.

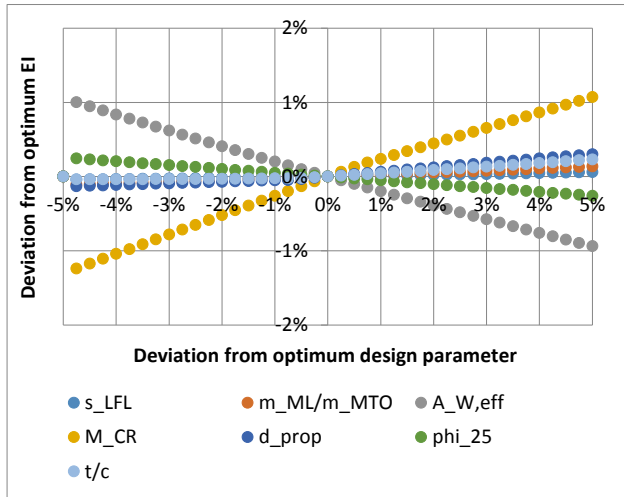


Fig. 15 Robustness analysis of the design parameters

Fig. 16 also shows an analysis of the robustness of the optimum design. In contrast to the robustness analysis presented in Fig. 15, all seven design parameters have been randomly varied together in a range between - 5 % ... + 5 % of the optimum value. Each point in the Figure represents a feasible aircraft design with its respective deviation from the optimum EI. It can be seen that the deviation from the optimum EI of all designs is within a range of about 0 % ... + 3.5 %.

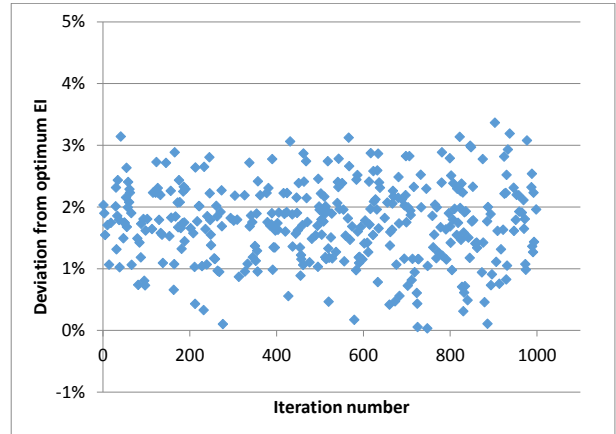


Fig. 16. Robustness analysis with a random variation of all design parameters

## 5 Trade-off between Environmental Impact and Direct Operating Costs

A Pareto front is used to analyze the trade-off between low EI and low DOC for the previously presented TA concept. It is investigated to what extent both objectives can be reached together and how much the DOC rise depending on the amount of EI improvement in order to determine the costs of better environmental protection for the aircraft operator.

Fig. 17 presents a Pareto front analysis for a fuel price of 1.32 USD/kg which has been assumed for the year 2030 as explained in Section 3. Each point in the Figure presents a feasible aircraft design. The scales show how many percent the designs are above the minimum reached EI and DOC. The Pareto front itself is visualized by a red line.

It can be seen that the EI of an aircraft solely optimized for minimum DOC (represented by the point on the y-axis) is only about 4 % higher than that of an aircraft solely optimized for minimum EI. On the other hand, the DOC of an aircraft solely optimized for minimum EI (represented by the point on the x-axis) are only about 3 % higher than those of an aircraft solely optimized for minimum DOC.

Fig. 18 presents the same Pareto front analysis as Fig. 17 but for a fuel price of 0.27 USD/kg which is the inflation-adjusted fuel price of 1988 when Airbus A320 had its entry into service. It can be seen that the EI of an aircraft solely optimized for minimum DOC is

about 8 % higher than that of an aircraft solely optimized for minimum EI. On the other hand, the DOC of an aircraft solely optimized for minimum EI are about 7 % higher than those of an aircraft solely optimized for minimum DOC.

It can be seen that the higher the fuel price, the more important the design for minimum fuel consumption and therefore EI independent of the weighting of DOC and EI in the design objective function. The lower the fuel price, the bigger the contrast between aircraft optimized for DOC and aircraft optimized for EI and therefore the higher the costs for better environmental protection.

The TA optimized for minimum EI (as presented in Section 3) is similar to a TA optimized for minimum DOC. This is because TA get their DOC advantages out of their low fuel consumption. Therefore TA with minimum DOC are similar to aircraft with minimum fuel consumption and minimum EI.

In contrast to that a DOC optimized turbofan aircraft compensates its higher fuel consumption by higher cruise speed. That is why the turbofan aircraft with minimum DOC differs more from that with minimum EI or in other words, the aircraft with minimum EI comes with higher disadvantages in DOC. To reach the objectives of low DOC and EI together, it makes therefore sense to choose TA instead of turbofan aircraft.

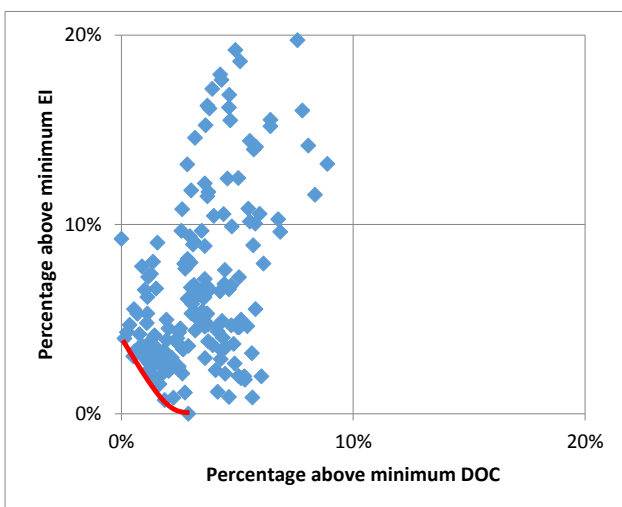


Fig. 17. Pareto front analysis for a fuel price of 1.32 USD/kg

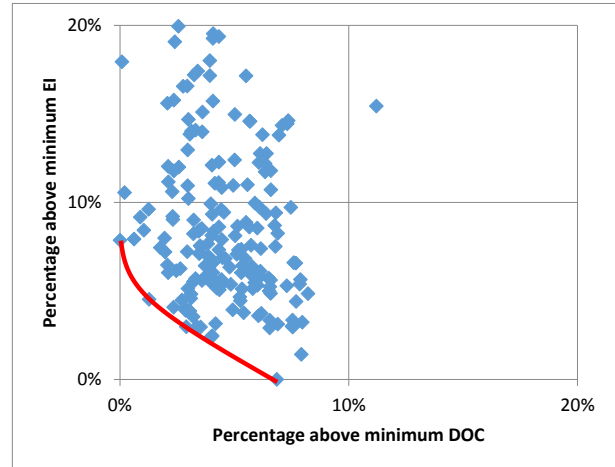


Fig. 18 Pareto front analysis for a fuel price of 0.27 USD/kg

## 6 Summary and Conclusion

This paper presented the influence of LCA on conceptual aircraft design using a medium range TA as design example. It is shown that EI could be reduced by about 46 % by solely designing aircraft for minimum EI. This is mainly reached by the use of turboprop engines combined with a high wing aspect ratio of almost 15, a very low cruise Mach number of 0.4 and the future technologies SBW and NLF. The reduced fuel consumption due to the use of these design parameters and features leads to additional snowball effects further reducing the mass and therefore fuel consumption of the aircraft.

On the selected DOC mission, the proposed aircraft still offers potential DOC improvements of about 12 % compared to the reference aircraft.

The presented aircraft design is based on single assumptions for important design parameters like fuel cost. Future work will amongst others concentrate on the influence of future scenarios on these design parameters and the design of the aircraft.

## Nomenclature

$A_{w,eff}$	Effective wing aspect ratio
$b_{w,geo}$	Geometrical span
$BPR$	Bypass-ratio
$c_{fuel}$	Fuel cost
$C_{D,0}$	Zero-lift drag coefficient

$d_{prop}$	Propeller diameter
$DOC$ (AEA)	Direct operating costs calculated using the method of the Association of European Airlines
$E_{max}$	Maximum glide ratio
$EIS$	Entry into service
$h_{ICA}$	Initial cruise altitude
$M_{CR}$	Cruise Mach number
$m_{F,trip}$	Fuel mass for the DOC range
$m_{ML}$	Maximum landing mass
$m_{MPL}$	Maximum payload mass
$m_{MTO}$	Maximum take-off mass
$m_{OE}$	Operating empty mass
$m_{PAX}$	Passenger mass
$m_{PL,DOC}$	Payload mass for the DOC calculation
$n_{PAX}$ (1-cl HD)	Number of passengers in a one class high-density layout
$P_{eq,ssl}$	Equivalent take-off power at static sea level
$PSFC$	Power specific fuel consumption
$R_{DOC}$	Range for the DOC calculation
$R_{MPL}$	Range at maximum payload
$S_{LFL}$	Landing field length
$S_{TOFL}$	Take-off field length
$S_W$	Wing area
$SP$	Seat pitch
$SS$	Single Score
$t_{TA}$	Turnaround time
$T_{TO}$	Take-off thrust
$t/c$	Wing thickness ratio
$U_{a,f}$	Utilization per year on DOC range
$\eta_{prop}$	Propeller efficiency during cruise
$\varphi_{25}$	Wing sweep at 25 % chord

### Acknowledgements

The authors acknowledge the financial support of the German Federal Environmental Foundation which made this work possible.

### References

- [1] European Commission. *Flightpath 2050 Europe's Vision for Aviation*. Luxembourg: Publications Office of the European Union, 2011. – ISBN: 978-92-79-19724-6. – URL: <http://ec.europa.eu/transport/air/doc/flightpath2050.pdf> (2014-06-17).
- [2] International Standard Organization. *Environmental management — Life cycle assessment — Principles and framework*. Second edition, July 2006.
- [3] Johannig, A and Scholz, D. *A First Step Towards the Integration of Life Cycle Assessment into Conceptual Aircraft Design*. In: *Publikationen zum DLRK 2013* (Deutscher Luft- und Raumfahrtkongress, Stuttgart, 10. - 12. September 2013).
- [4] Johannig, A and Scholz, D. *Novel Low-Flying Propeller-Driven Aircraft Concept For Reduced Direct Operating Costs And Emissions*. In: *CD Proceedings : ICAS 2012 - 28th Congress of the International Council of the Aeronautical Sciences* (ICAS, Brisbane, 23.-28. September 2012). Edinburgh, UK : Optimage Ltd, 2012. - ISBN: 978-0-9565333-1-9. Paper: ICAS2012-1.10.5 (510.PDF). URL: [http://www.icas.org/ICAS\\_ARCHIVE/ICAS2012/ABSTRACTS/510.HTM](http://www.icas.org/ICAS_ARCHIVE/ICAS2012/ABSTRACTS/510.HTM) (2014-06-17).
- [5] AIRBUS S.A.S.. *A320/A320Neo AIRPLANE CHARACTERISTICS AIRPORT AND MAINTENANCE PLANNING*. Issue: Sep 30/85, Rev: May 01/14. – URL: [http://www.airbus.com/fileadmin/media\\_gallery/files/tech\\_data/AC/Airbus-AC\\_A320\\_May2014.pdf](http://www.airbus.com/fileadmin/media_gallery/files/tech_data/AC/Airbus-AC_A320_May2014.pdf) (2014-06-17).
- [6] URL: [http://www.aerospaceweb.org/aircraft/jetliner/a320/a320\\_schem\\_01.jpg](http://www.aerospaceweb.org/aircraft/jetliner/a320/a320_schem_01.jpg) (2014-06-17)
- [7] Scholz, D. *Skript zur Vorlesung Flugzeugentwurf*. Hamburg, Fachhochschule Hamburg, FB Fahrzeugtechnik, Abt. Flugzeugbau, Vorlesungsskript, 1999. – URL: <http://FE.ProfScholz.de> (2014-06-30).
- [8] Scholz, D. *DOC-Assessment Method*. TU Berlin – *DOC Method*. J. Thorbeck. Presentation (3<sup>rd</sup> Symposium on Collaboration in Aircraft Design, Linköping, 19.09.2013). Sweden. 2012. URL: [http://www.fzt.haw-hamburg.de/pers/Scholz/Aero/TU-Berlin\\_DOC-Method\\_with\\_remarks\\_13-09-19.pdf](http://www.fzt.haw-hamburg.de/pers/Scholz/Aero/TU-Berlin_DOC-Method_with_remarks_13-09-19.pdf) (2013-06-28)
- [9] International Civil Aviation Organization. *Aerodromes, Volume I – Aerodrome Design and Operations*. Annex 14 to the Convention on International Civil Aviation, 5th edition, 2009.
- [10] Association of European Airlines. *Short-Medium Range Aircraft AEA Requirements*. Brussels, AEA, 1989. (G(T)5656).

## Copyright Statement

The authors confirm that they, and/or their company or organization, hold copyright on all of the original material included in this paper. The authors also confirm that they have obtained permission, from the copyright holder of any third party material included in this paper, to publish it as part of their paper. The authors confirm that they give permission, or have obtained permission from the copyright holder of this paper, for the publication and distribution of this paper as part of the ICAS 2014 proceedings or as individual off-prints from the proceedings.